

# A quantitative fluorescence-based steady-state assay of DNA polymerase

Max D. Driscoll, Julius Rentergent and Sam Hay

Manchester Institute of Biotechnology and Faculty of Life Sciences, University of Manchester, UK

## Keywords

DNA quantification; enzyme kinetics; fluorescence; Michaelis–Menten; PicoGreen; polymerase; steady-state

## Correspondence

S. Hay, Manchester Institute of Biotechnology and Faculty of Life Sciences, University of Manchester, 131 Princess Street, Greater Manchester M1 7DN, UK  
Fax: +44 0 161 306 5201  
Tel: +44 0 161 306 5141  
E-mail: sam.hay@manchester.ac.uk

(Received 13 August 2013, revised 12 January 2014, accepted 18 February 2014)

doi:10.1111/febs.12760

Fluorescent dyes that bind DNA have been demonstrated as a useful alternative to radionucleotides for the quantification of DNA and the *in vitro* measurement of the activity of DNA polymerases and nucleases. However, this approach is generally used in a semi-quantitative way to determine relative rates of reaction. In this report, we demonstrate a method for the simultaneous quantification of DNA in both its single-strand and double-strand forms using the dye PicoGreen. This approach is used in a steady-state assay of DNA polymerase Klenow fragment  $exo^-$ , where we determine  $k_{cat}$  and  $K_m$  values for the DNA polymerase that are in excellent agreement with literature values.

## Introduction

The importance of DNA polymerase enzymes in both biology and biotechnology cannot be understated. Central to DNA replication and repair in all living organisms, polymerases have been studied for decades [1]. Research into DNA polymerase kinetics dates back to the 1970s and 1980s and has typically used primer-extension assays [2–6] or stopped or quench-flow pre-steady-state methods [7–11] (for a review see [12]). This has led to the employment of this group of enzymes in everyday laboratory protocols and techniques such as PCR and its derivatives and DNA sequencing. However, much of the kinetic characterization of DNA polymerase enzymes has historically relied on the use of radiological methods, which are now being phased out due to the inherent risks associated with the use of radioisotopes. Alternative methods are being adopted, frequently employing fluorescence detection [13–18], but these are often, at best, semi-quantitative. For example, while it is

possible, during a real-time PCR reaction, to observe when a desired reaction has reached completion, and to make comparisons between different reactions, extracting reliable kinetic parameters (i.e. rate constants) is generally not possible. The utilization of fluorescent dyes to quantify DNA and to assay polymerase activity has been well established since the 1960s [19–21]. Fluorescent nucleotide analogues have also been used to study DNA structure and polymerase mechanisms [22,23]. However, to the best of our knowledge, these methods have not been employed in a simple assay for the elucidation of steady-state kinetic parameters (i.e.  $k_{cat}$  and  $K_m$ ) which facilitates comparison with other kinetic studies performed using alternative approaches.

PicoGreen (PG) is a commercially available fluorescent dye that is often used for the quantification of dsDNA [24–28]. It is similar in properties and structure to SYBR green [29], which has been used for

## Abbreviations

KF, Klenow fragment of DNA polymerase I; PG, PicoGreen.

many years to quantify DNA in such techniques as real-time PCR and quantitative PCR [30–33]. Fluorescent dyes have been shown to bind to DNA in a variety of different ways [34]. PG has been shown both to intercalate into the double helix of DNA with a frequency of approximately one dye molecule per four base pairs of dsDNA and also to bind along the phosphate backbone surface using electrostatic interactions along with groove binding [35]. PG displays high affinity to DNA, which lends itself to a large linear dynamic range. The fluorescence enhancement of PG upon association with dsDNA has been reported to be ~2000-fold and detection of DNA concentrations ranging from low picomolar to micromolar by PG has been demonstrated as the  $K_d$  for PG/DNA is in the nanomolar range (dependent upon buffer conditions) [34–36]. The fluorescence enhancement of PG when bound to ssDNA is significantly less than that when bound to dsDNA and the fluorescence sensitivity to dsDNA is not greatly affected by the presence of ssDNA [36]. As a result, PG lends itself to studying the production of dsDNA from a single-stand template, and therefore also to the study of DNA polymerase activity. Indeed, a PG-based DNA polymerase assay has been demonstrated, but this approach has not yet progressed beyond the qualitative or comparative analysis of dsDNA production [14,15]. Similarly, PG has also been employed to semi-quantitatively monitor the hydrolysis of dsDNA catalysed by DNA nuclease [37].

In this report, we present a fluorescence-based assay for the study of DNA polymerase kinetics based on the selective detection of dsDNA by PG. We focus on the steady-state turnover of Klenow fragment (KF)  $\text{exo}^-$ , which is a well-characterized model polymerase [2,3,38–44]. We have designed the assay to simplify the study of polymerases, with the removal of nucleotide analogues

## Results and discussion

In order to monitor dsDNA production during a polymerase assay using a fluorophore such as PG, the fluorescence from PG bound to dsDNA ( $f_{ds}$ ) must be deconvoluted from the total observed fluorescence from the sample,  $f_{obs}$ :

$$f_{obs} = f_{PG}[PG] + f_{dNTP}[PG \cdot dNTPs] + f_{ds}[PG \cdot dsDNA] + f_{ss}[PG \cdot ssDNA] \quad (1)$$

Under the instrumental and buffer conditions used throughout this study (given in Materials and methods), we measured  $f_{PG} = 0.85 \pm 0.23$  counts per second (cps) per nM PG. By titrating dNTP into a solution of 3  $\mu\text{M}$  PG (the PG concentration typically used throughout this study), a value of  $f_{dNTP} = 0.050 \pm 0.002$  cps·(nM dNTP) $^{-1}$  was determined (data not shown). Next, 50-mers of dsDNA and ssDNA were titrated into 3  $\mu\text{M}$  PG to determine  $f_{ds} = 580 \pm 18$  cps·(nM dsDNA) $^{-1}$  and  $f_{ss} = 36 \pm 2$  and  $50 \pm 3$  cps·(nM ssDNA) $^{-1}$  (Fig. 1). The dsDNA was made by annealing a 1 : 1 ratio of T7pR30 : T7pR30rc (Table 1) and the different values of  $f_{ss}$  are for the T7pR30 and T7pR30rc oligonucleotides, respectively. The variability in  $f_{ss}$  suggests that the magnitude of the fluorescence enhancement upon DNA binding to PG may have some sequence dependence.

The differential fluorescence enhancement of PG bound to dsDNA versus ssDNA ( $f_{ds}/f_{ss}$ ) observed in Fig. 1B is 11–16, which is of the same order as previously reported [36]. To alternatively determine  $f_{ds}$  and  $f_{ss}$  under conditions similar to those used during a polymerase assay, one ssDNA 50-mer (T7pR50; Table 1) was titrated (with annealing) against its reverse complement (T7pR50rc). These data, shown in Fig. 2, were fitted to a quadratic function (Eqn 2) to simultaneously determine  $f_{ds}$  and  $f_{ss}$ .

$$\begin{aligned} f_{obs} &\approx f_{ds}[\text{dsDNA}] + f_{ss}[\text{ssDNA}] \\ [\text{dsDNA}] &= \{length/2\} \left\{ ([O_1] + [O_2] + K_d) - \sqrt{([O_1] + [O_2] + K_d)^2 - 4[O_1][O_2]} \right\} \\ [\text{ssDNA}] &= length([O_1] + [O_2]) - [\text{dsDNA}] \end{aligned} \quad (2)$$

and the need to visualize results, indirectly, using gel electrophoresis. This assay can be used to obtain steady-state parameters such as the apparent Michaelis–Menten constant ( $K_m$ ) and, as it is quantitative, the velocities  $V_{max}$  and  $k_{cat}$ . The assay consumes relatively small quantities of DNA, nucleotides and enzyme and can be performed using a conventional fluorometer, simply first requiring the creation of a standard curve.

Here, *length* is the ssDNA (oligonucleotide) length (i.e. 50) and  $[O_1]$  and  $[O_2]$  are the concentrations of the T7pR50 and T7pR50rc oligonucleotides.  $f_{dNTP}$  and  $f_{PG}$  can also be omitted in the approximation of  $f_{obs}$  as their contributions are negligible. Fitting the data in Fig. 2B yielded  $f_{ds} = 562 \pm 9$  cps·nM $^{-1}$ ,  $f_{ss} = 53 \pm 2$  cps·nM $^{-1}$  and  $K_d = 2.9 \pm 0.7$  nM. These values are

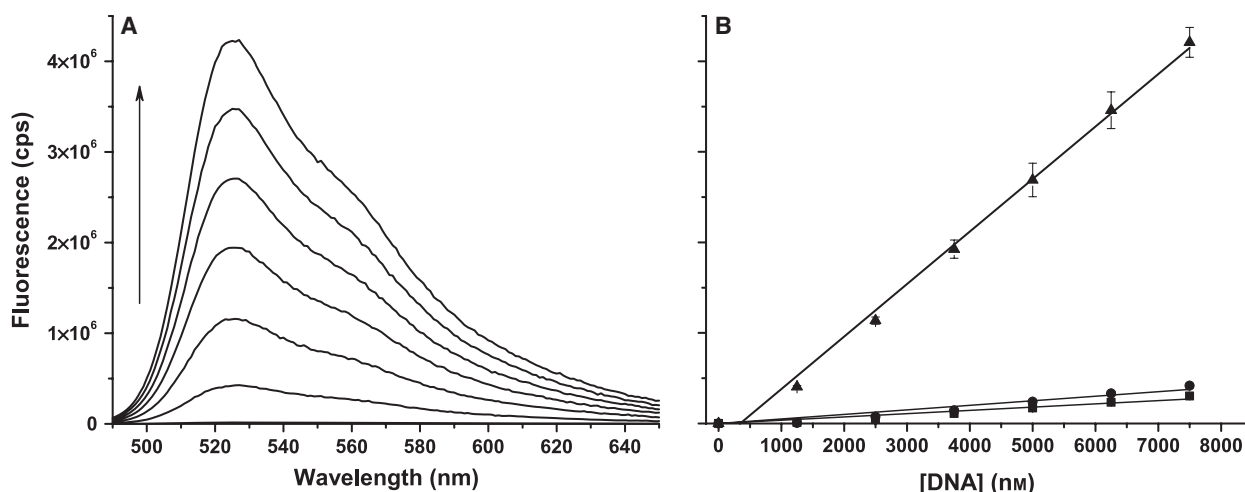


**Fig. 1.** dsDNA and ssDNA quantification using PG. (A) Selected fluorescence emission spectra (excitation at 480 nm) as dsDNA (1 : 1 T7pR30 : T7pR30rc) is titrated into 3  $\mu$ M PG. The arrow highlights the increase in emission at 525 nm with increasing [dsDNA]. (B) The dependence of the peak fluorescence emission at 525 nm on [dsDNA] (triangles) and [ssDNA] (T7pR30, circles; T7pR30rc, squares). Note that the DNA concentration is expressed in nM of nucleotides or base pairs (i.e. concentration of oligonucleotide  $\times$  length). The data shown are averages of triplicate data sets and, using the standard deviations as errors, were fitted (excluding those at the origin) to a linear function to extract the  $f_{ds}$  and  $f_{ss}$  values given in the text. Note that while the data in (B) do not go through the origin – the linear dynamic ranges do not extend to [DNA] = 0 – this effect is not observed under assay conditions, as shown in Fig. 2.

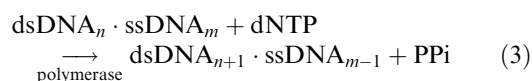
**Table 1.** ssDNA oligonucleotide templates used in this work. The complementary sequences for the T7 primer are in bold and the T7 sequence in the reverse complement 50-mer (T7pR30rc) is shown underlined. The nomenclature for the oligonucleotides refers to the T7 promoter sequence and the length of the random polynucleotide region of 30–100 nucleotides.

Oligonucleotide	Length	Sequence
T7pR30	50	5'–TAC GGA TCC ATG CTA GTC CAT TAG CAG GTG <b>CCC TAT AGT GAG TCG TAT TA</b> –3'
T7pR50	70	5'–GTG GAC AGT CTG GTA TGT AGT CAG GCT CCA GGA GTC GCC TAT GCC AAC CTC <b>CCT ATA GTG AGT CGT ATT A</b> –3'
T7pR80	100	5'–GTA GCT GAC TTC TTC ACC ACA TCT ACC AAA GTG GGC AGT CTG GTA TGC AGT CAG GCT CCA GGA GTC GCC TAT GCC AAC <b>CTC CCT ATA GTG AGT CGT ATT A</b> –3'
T7pR100	120	5'–GAC TCG AAT GTG ACT CAG TGA TAG CTG ACT TCT TCA CCA CAT CTA CCA AAG TGG GCA GTC TGG TAT GCA GTC AGG CTC CAG GAG TCG CCT ATG CCA ACC <b>TCC CTA TAG TGA GTC GTA TTA</b> –3'
T7pR30rc	50	5'– <u>TAA TAC GAC TCA CTA TAG GGC ACC TGC TAA TGG ACT AGC ATG GAT CCG TA</u> –3'

comparable to those determined in Fig. 1 and yield  $f_{ds}/f_{ss} = 10.6 \pm 0.1$ . The observed  $K_d$  is in good agreement with previous reports [34–36]. Consequently PG can be used to discriminate between dsDNA and ssDNA. The difference in fluorescence emission between PG bound to dsDNA and ssDNA ( $\sim 11$ -fold) is consistent between experiments. This is important to consider, as it has been shown that this difference in fluorescence enhancement is dependent upon buffer conditions [36].

The data in Figs 1 and 2 show that it is possible to accurately determine the concentration of dsDNA or ssDNA in reaction mixtures containing dsDNA, ssDNA and PG if the concentration of the other spe-

cies is known. However, if we consider an idealized polymerase-catalysed reaction (Eqn 3), ssDNA and dNTPs are stoichiometrically converted to dsDNA.



The change in  $f_{obs}$  as the reaction progresses ( $\Delta f_{obs}$ ) then allows the determination of the amount of dsDNA produced ( $\Delta[\text{dsDNA}]$ ) without knowledge of the concentration of any of the species:

$$\Delta f_{obs} \approx (f_{ds} - f_{ss})\Delta[\text{dsDNA}] = f_{\Delta}\Delta[\text{dsDNA}] \quad (4)$$

We will use a value of  $f_{\Delta} = 520 \pm 30 \text{ cps}\cdot\text{nm}^{-1}$ , which was determined using  $f_{ds}$  and  $f_{ss}$  values averaged

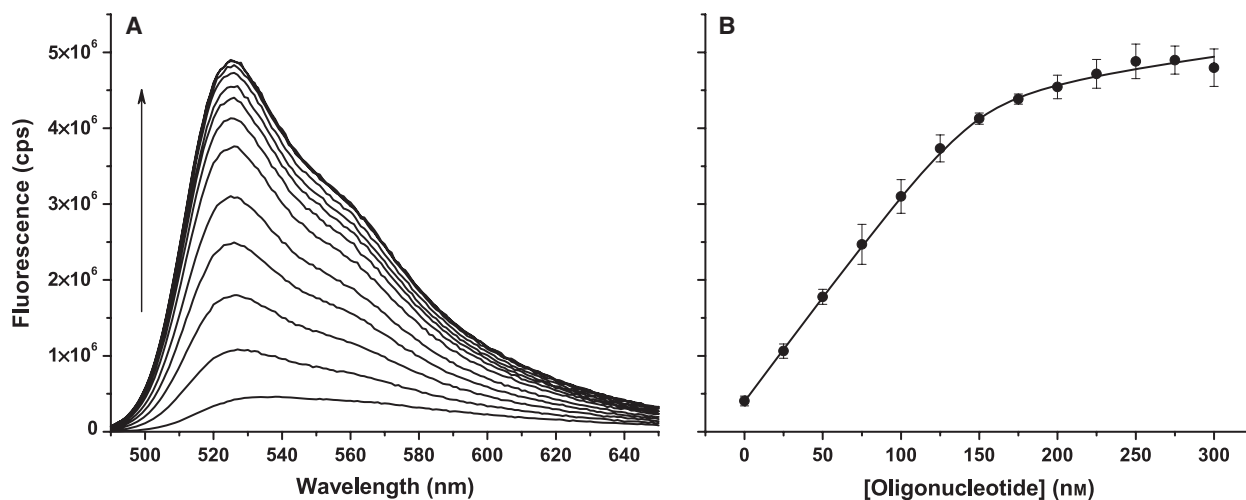


**Fig. 2.** dsDNA and ssDNA discrimination using PG. (A) Fluorescence emission spectra as the ssDNA 50-mer T7pR30 is titrated into 150 nM of its reverse complement (T7pR30rc) in the presence of excess (3  $\mu\text{M}$ ) PG. (B) The fluorescence at 525 nm versus [T7pR30]. The data shown are averages of triplicate data sets, using the standard deviations as errors, and are fitted to Eqn (2), with more detail given in the text.

between those determined in Figs 1 and 2. While this value will vary depending on the fluorometer and instrument parameters employed, it can be readily determined using the method described in Fig. 1 and/or Fig. 2. Note that if absolute values of  $V_{\text{max}}$  and  $k_{\text{cat}}$  are not required, then relative velocities can be readily determined by comparison with a reference reaction. This removes the necessity of the creation of a standard curve to determine  $f_{\Delta}$  in Eqn (4).

The rate of dsDNA produced during steady-state turnover of KF  $\text{exo}^-$  was initially investigated using a continuous assay with a saturating concentration (1 mM) of dNTPs and 100 nM of the T7pR30 template with a two-fold excess of T7 primer annealed. With annealed T7 primer, the T7pR30 template has a 5' overhang of 30 nucleotides that can be filled in during the reaction. The assay was performed in the presence of PG and the change in [dsDNA] was quantified by monitoring the fluorescence emission from PG at 525 nm. PG was found to strongly inhibit the reaction with an apparent  $K_{\text{I}} = 30 \pm 8$  nM (Fig. 3). It is notable that this value is of the same order as the  $K_{\text{d}}$  reported for DNA binding to PG [34,36] and of that determined in Fig. 2. Similar inhibition has been reported previously [14] and can be rationalized if polymerase binding to the template DNA is inhibited when template DNA has bound PG present; essentially, PG appears to be acting like a competitive inhibitor. While it may be possible to perform continuous assays in the presence of low concentrations (sub- $\mu\text{M}$ ) of PG, this is problematic. In order for PG to linearly report on [dsDNA], it must be saturating

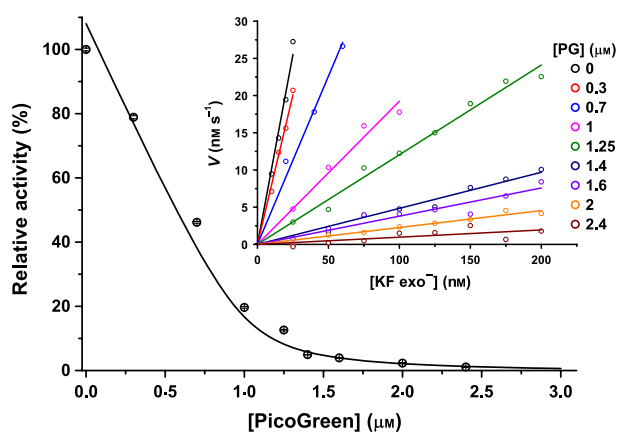


**Fig. 3.** Steady-state turnover in the presence of PG. The observed rate of steady-state turnover of KF  $\text{exo}^-$  with 100 nM template DNA (1 : 2 T7pR30 : T7 primer) and 1 mM dNTPs in the presence of increasing PG at room temperature. Reactions containing 0, 0.3 and 0.7  $\mu\text{M}$  PG were performed using the stopped method in Fig. 4 with the PG concentration made up to 3  $\mu\text{M}$  immediately prior to measurement (to ensure sufficient PG to report on all the dsDNA produced). All other reactions were performed continuously. The inset shows the dependence of observed  $V$  on [KF  $\text{exo}^-$ ]. These data were each fitted to a linear function (solid lines) to determine the data shown in the main panel. The [PG] dependence of the activity is fitted to a quadratic function (solid line) with an apparent  $K_{\text{I}} = 30 \pm 8$  nM at a saturating concentration of  $1.0 \pm 0.1$   $\mu\text{M}$  PG.

relative to the final amount of dsDNA produced. With 100 nM of a 50-mer template (as in Fig. 3), a minimum PG concentration of 1.25  $\mu\text{M}$  is required to allow PG to bind, on average, to every fourth base pair of dsDNA [35]. If a longer template is used (see later),

then more PG is required and/or the concentration of template must be reduced, which reduces the sensitivity of the assay. This is also assuming that intercalation is the largest contributor to fluorescence enhancement/emission, given that PG can also associate with DNA via electrostatics and groove binding [35].

As an alternative to optimizing the conditions of the continuous assay, a stopped assay was explored. The reaction conditions were similar to those used in Fig. 3 and typically contained 10 or 100 nM primed template and 0–500  $\mu\text{M}$  dNTPs. The reaction was initiated by the addition of 5 or 50 nM KF  $\text{exo}^-$  and aliquots were quenched by the addition of 3  $\mu\text{M}$  PG at 10 s intervals. We used PG to quench the reaction as EDTA (a common polymerase quencher) was found to reduce the fluorescence of PG/DNA solutions. This is most probably due to EDTA sequestering metal ions (i.e.  $\text{Mg}^{2+}$ ), which have been shown to enhance PG fluorescence [45,46]. No activity was measured with 3  $\mu\text{M}$  PG in Fig. 3, and care was taken during the stopped assay to minimize the time between quenching and fluorescence measurement. The stopped assay with T7pR30 template is shown in Fig. 4. The reaction progress curves show the reaction going to completion with higher dNTP concentrations. In these cases, the template is limiting and the reaction stops when the single-strand 5' overhang of the template is filled in. This was confirmed by performing assays with progressively longer templates with 50, 80 and 100 nucleotides of 5' overhang (Table 1; data not shown). These data

showed the reaction saturating after increasingly longer intervals, with correspondingly longer linear regions and higher final fluorescence levels. One additional advantage of a stopped assay is that the concentration of the reaction can be diluted upon quenching in order to ensure that PG is saturating. Thus, it is possible to use longer templates without compromising the sensitivity of the assay.

As the progress curves measured are non-linear, these data were fitted to a quadratic function to extract the initial velocities (Eqn 5) with example fits shown in Fig. 4B.

$$\Delta f = (V_{\text{initial}}/2) \left\{ (c + t_{\text{sat}} + t) - \sqrt{(c + t_{\text{sat}} + t)^2 - 4t_{\text{sat}}t} \right\} \quad (5)$$

Equation (5) provides a model-free method of fitting non-linear time course data in order to determine the slope of the initial linear region, i.e.  $V_{\text{initial}}$ . The  $t_{\text{sat}}$  and  $c$  parameters are phenomenological and describe the time when the reaction has saturated ( $\sim 60$  s in Fig. 4B) and the curvature around this point, respectively.

The initial velocity data show a hyperbolic dependence of the observed velocity on dNTP concentration (Fig. 5). By fitting these data to a Michaelis–Menten expression (Eqn 6), apparent  $V_{\text{max}}$  and  $K_{\text{m}}$  values were determined for each of the four templates (Fig. 5; Table 2).

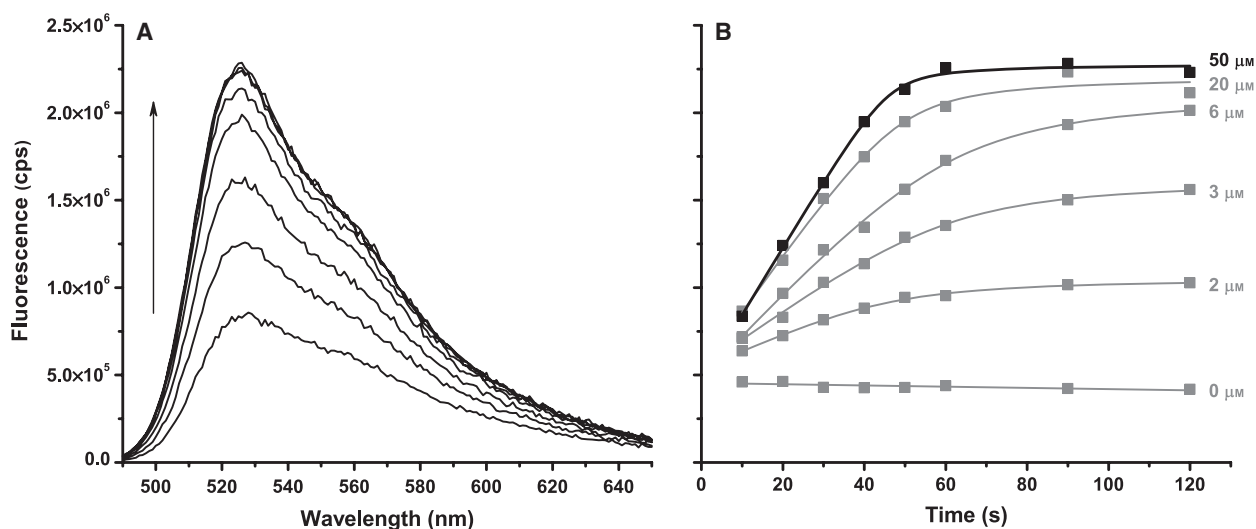


**Fig. 4.** Stopped steady-state assay. (A) Fluorescence emission spectra obtained during a stopped steady-state assay of KF  $\text{exo}^-$  with T7pR30. The spectra correspond to the 50  $\mu\text{M}$  data in (B) shown in black. (B) Reaction progress curves measured using the fluorescence maxima at each time point and dNTP concentration (as labelled). All measurements were performed with 50 nM KF  $\text{exo}^-$  and 100 nM 1 : 1.2 T7pR30 : T7 primer (annealed) at room temperature.

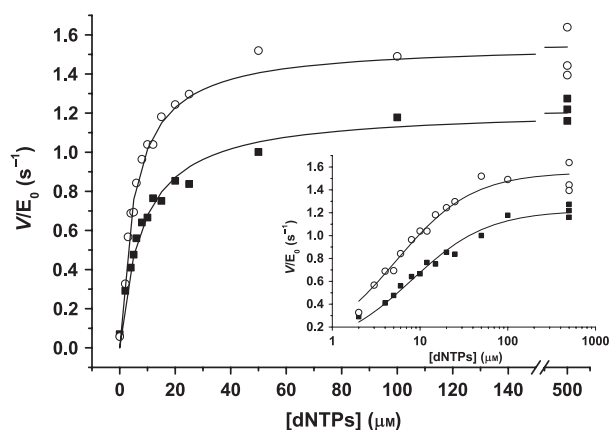


**Fig. 5.** Michaelis–Menten steady-state data. The dNTP dependence of the observed initial reaction velocity data extracted from stopped assays of KF  $\text{exo}^-$  (50 nM) with 100 nM T7pR50 (circles) and T7pR100 (squares) templates. The inset shows the same data on a log concentration axis and the data are fitted to Eqn (6) with fitted values given in Table 2.

**Table 2.** Apparent Michaelis–Menten parameters derived from fits of Eqn (6) (with fitting errors) to stopped steady-state assays of the dNTP dependence of KF  $\text{exo}^-$  with 50 nM template.

Template	$k_{\text{cat}}$ ( $\text{s}^{-1}$ )	$K_m$ ( $\mu\text{M}$ )	$k_{\text{cat}}/K_m$ ( $\mu\text{M}^{-1}\cdot\text{s}^{-1}$ )
T7pR30	$1.43 \pm 0.05$	$4.2 \pm 0.6$	$0.34 \pm 0.06$
T7pR50	$1.55 \pm 0.03$	$5.3 \pm 0.5$	$0.29 \pm 0.03$
T7pR80	$0.93 \pm 0.03$	$2.8 \pm 0.5$	$0.33 \pm 0.07$
T7pR100	$1.22 \pm 0.02$	$8.0 \pm 0.6$	$0.15 \pm 0.02$

$$V_{\text{obs}} = V_{\text{max}}[\text{dNTP}]/(K_m + [\text{dNTP}]) \quad (6)$$

As template was in excess over enzyme in these experiments, apparent  $k_{\text{cat}}$  values were determined by dividing  $V_{\text{max}}$  by the concentration of polymerase. While there is some variability in the measured  $k_{\text{cat}}$  and  $K_m$  values, they are similar to literature values reported using steady-state methods [4,47]. Interestingly,  $k_{\text{cat}}/K_m$ , which is a measure of productive dNTP capture, is significantly less variable. The variability in  $k_{\text{cat}}$  and  $K_m$  values may arise due to sequence variations between our templates. In our experiments, 30–100 nucleotides of dsDNA were synthesized (depending on the template) when the assay was allowed to go to completion.

The dependence of the T7pR80 template concentration on the stopped assay was next explored by performing the assay with saturating dNTPs (500  $\mu\text{M}$ ). KF  $\text{exo}^-$  was used at 5 nM to allow sufficient time to acquire a reasonable reaction time course (data not shown). These data were again fitted to Eqn (5) to extract initial velocities that were then fitted to a

‘tight-binding’ expression (Eqn 7;  $[E]_0$  is the initial enzyme concentration) to extract apparent  $V_{\text{max}}$  and  $K_m$  values for DNA binding to the polymerase (Fig. 6).

$$V = (V_{\text{max}}/2[E]_0) \left\{ ([E]_0 + [\text{dsDNA}]_0 + K_m) - \sqrt{([E]_0 + [\text{dsDNA}]_0 + K_m)^2 - 4[E]_0[\text{dsDNA}]_0} \right\} \quad (7)$$

Values of  $V_{\text{max}} = 1.6 \pm 0.2 \text{ s}^{-1}$  and  $K_m = 7 \pm 3 \text{ nM}$  were determined from the data in Fig. 6.

Finally, the dependence of the KF  $\text{exo}^-$  concentration on the stopped assay was investigated with 50 nM T7pR100 template and saturating dNTPs (500  $\mu\text{M}$ ). It became progressively more difficult to extract reliable initial velocities from the time courses as the enzyme concentration was increased, as the reaction reached completion more quickly (Fig. 7, inset). The enzyme concentration dependence on the observed velocity appears to show saturation behaviour (Fig. 7) and these data were fitted to Eqn (7) to determine apparent  $V_{\text{max}} = 2.9 \pm 0.3 \text{ s}^{-1}$  and  $K_m = 22 \pm 10 \text{ nM}$  values. It is interesting to note that the apparent  $K_m$  values determined from Figs 6 and 7, respectively, are not significantly different and are similar to values determined for the association of KF with DNA using pre-steady-state methods [3]. It may be possible to study the processivity of the DNA polymerase using this assay, but a rapid-quench approach is likely to be required if significantly shorter templates are to be used.

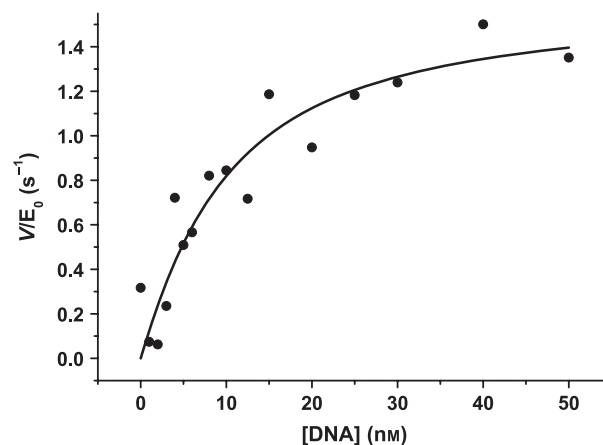


**Fig. 6.** Pseudo-Michaelis–Menten steady-state data. The T7pR80 template DNA dependence of the observed initial reaction velocity data extracted from stopped assays of 5 nM KF  $\text{exo}^-$  with 500  $\mu\text{M}$  dNTPs. The data are fitted to Eqn (7) ( $E_0 = 5 \text{ nM}$ ) to obtain  $V_{\text{max}} = 1.6 \pm 0.2 \text{ s}^{-1}$  and  $K_m = 7 \pm 3 \text{ nM}$ .

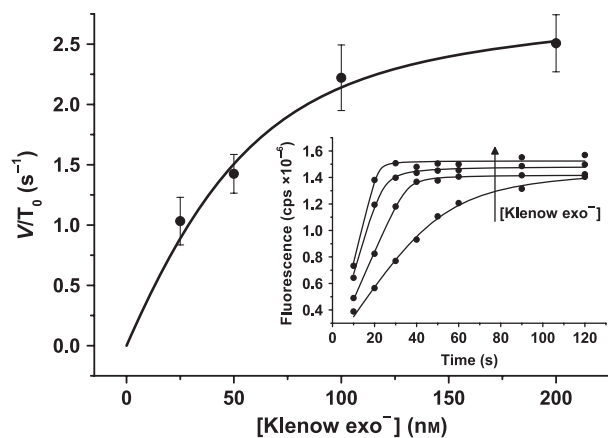


**Fig. 7.** Pseudo-Michaelis–Menten steady-state data. The enzyme (KF  $\text{exo}^-$ ) dependence of the observed initial reaction velocity data extracted from stopped assays with 50 nM T7pR100 template and 500  $\mu\text{M}$  dNTPs. The data are fitted to Eqn (7) ( $T_0 = 50$  nM) to obtain  $V_{\text{max}} = 2.9 \pm 0.3 \text{ s}^{-1}$  and  $K_m = 22 \pm 10$  nM. The inset shows the time course of the experiments performed with 25, 50, 100 and 200 nM KF  $\text{exo}^-$ . These data are fitted to Eqn (5) in order to extract the  $V_{\text{obs}}$  values plotted in the main panel.

In order for an enzyme reaction to be at steady-state, it has been argued that the following condition,  $\epsilon$ , must be met:  $\epsilon = E_0/(K_m + S_0) \ll 1$  [48]. While this criterion may not be strictly valid for non-Michaelis–Menten mechanisms such as that of DNA polymerase (which is multi-step and effectively has two substrates), it can still aid in the interpretation of enzyme turnover data. The dNTP dependences (Fig. 4; Table 2) were measured under conditions where  $\epsilon < 0.01$ , while the template and enzyme dependences were, by necessity, measured with  $0.08 < \epsilon < 0.7$  and  $0.3 < \epsilon < 3.2$ , respectively. Consequently, it would appear that our assay is capable of measuring steady-state turnover of DNA polymerase but only for nucleotide incorporation. This is likely to be a problem for other steady-state assays, and it is interesting to note that the value of  $k_{\text{cat}}$  determined in Fig. 6 is similar to those determined from the dNTP dependences (Table 2).

In this report, we have demonstrated a quantitative steady-state kinetic assay of the stoichiometric conversion of ssDNA to dsDNA catalysed by DNA polymerases, based on the differential fluorescence of PG when bound to dsDNA and ssDNA. PG was found to be a potent inhibitor of the KF  $\text{exo}^-$  reaction with an apparent inhibition constant of  $\sim 30$  nM. However, by performing a stopped assay, Michaelis–Menten parameters ( $k_{\text{cat}}$ ,  $K_m$ ,  $k_{\text{cat}}/K_m$ ) for DNA polymerase KF  $\text{exo}^-$  were determined and found to be in good agreement with previously reported values. The assay was found to be reliable over a range of DNA, enzyme and nucleotide concentrations and offers a viable alternative to

conventional kinetic assays of DNA polymerase that employ radionucleotides. We also see no reason why this stopped assay cannot be applied to other DNA polymerase enzymes (and possibly reverse transcriptase enzymes), although the inhibition of the enzyme by PG should be confirmed first or an alternative quencher used. By employing a fluorescence plate reader, it is anticipated that a full steady-state assay of an enzyme could be performed in a few minutes. This could then lead to a screening assay, not only to examine enzyme kinetics, but potentially also to look at, for example, polymerase inhibitors.

## Materials and methods

KF  $\text{exo}^-$  and NEB buffer 2 (10 mM Tris/HCl, 50 mM NaCl, 10 mM  $\text{MgCl}_2$ , 1 mM dithiothreitol, pH 7.9) were obtained from New England Biolabs (Hitchin, Hertfordshire, UK). KF  $\text{exo}^-$  was monitored between batches by SDS/PAGE (single band at  $\sim 68$  kDa) and its concentration was determined spectrophotometrically ( $\epsilon_{280} = 55\,450 \text{ M}^{-1}\text{cm}^{-1}$ ) [43,44]. dNTPs were obtained from Peqlab Ltd (Sarisbury Green, Hampshire, UK). PG was obtained from Invitrogen (Life Technologies, Paisley, UK) and its concentration was determined by  $\epsilon_{500} = 70\,000 \text{ M}^{-1}\text{cm}^{-1}$  [36]. PG was always used at a concentration below 4  $\mu\text{M}$  for fluorescence experiments to avoid inner filter effects.

HPLC-purified DNA oligonucleotides were obtained from Eurofins MWG Operon (London, UK) and their sequences are given in Table 1. The sequences are designed to anneal to the T7 primer (from the T7 promoter sequence, explaining their nomenclature), leaving a 30–100 nucleotide 5' overhang. This region of ssDNA is randomized and has approximately equal ratios of A : T : C : G. No secondary structure is predicted in any of the sequences. Oligonucleotides were annealed by heating the mixture to 95  $^{\circ}\text{C}$  for 10–15 min in buffer 2 (see below) before cooling to room temperature over at least 45 min. Unless stated otherwise, primed templates used for steady-state kinetics were made using a template oligo : T7 primer ratio of 1 : 1.2.

Fluorescence measurements were performed with an Edinburgh Instruments FLS920 spectrometer (Edinburgh, UK) with a 450 W xenon arc lamp light source, double excitation and emission monochromators and a red-sensitive cooled photomultiplier detector. Quartz fluorescence cells (Starna Scientific Ltd, Hainault, UK) with a 100  $\mu\text{L}$  cell volume and 10 mm excitation pathlength were used. All measurements were performed at room temperature ( $\sim 23$   $^{\circ}\text{C}$ ). Care was taken to minimize photobleaching of PG by minimizing the excitation energy using a 0.5 nm excitation slit width. For all measurements, a 5 nm emission slit width and 0.1 s averaging time were used when acquiring spectra.

Steady-state reactions were performed in NEB buffer 2. The standard assay consisted of 100 nM DNA template, 5

or 50 nM polymerase and equal quantities of each dNTP (combined concentrations are given in the text). Reactions were typically initiated by the addition of the polymerase. Discontinuous assays were stopped with 3  $\mu$ M PG and measurements were made within 10 min of stopping. No significant change in fluorescence was observed upon waiting longer before measurement.

## Acknowledgements

This work was funded by the UK British Biological Sciences Research Council (BBSRC) and SH is a BBSRC David Phillips Fellow.

## References

- Lehman IR, Bessman MJ, Simms ES & Kornberg A (1958) Enzymatic synthesis of deoxyribonucleic acid. I. Preparation of substrates and partial purification of an enzyme from *Escherichia coli*. *J Biol Chem* **233**, 163–170.
- Bryant FR, Johnson KA & Benkovic SJ (1983) Elementary steps in the DNA polymerase I reaction pathway. *Biochemistry* **22**, 3537–3546.
- Kuchta RD, Mizrahi V, Benkovic PA, Johnson KA & Benkovic SJ (1987) Kinetic mechanism of DNA polymerase I (Klenow). *Biochemistry* **26**, 8410–8417.
- Polesky AH, Steitz TA, Grindley ND & Joyce CM (1990) Identification of residues critical for the polymerase activity of the Klenow fragment of DNA polymerase I from *Escherichia coli*. *J Biol Chem* **265**, 14579–14591.
- Richardson CC, Schildkraut CL, Aposhian HV & Kornberg A (1964) Enzymatic synthesis of deoxyribonucleic acid. XIV. Further purification and properties of deoxyribonucleic acid polymerase of *Escherichia coli*. *J Biol Chem* **239**, 222–232.
- Bertram JG, Oertell K, Petruska J & Goodman MF (2010) DNA polymerase fidelity: comparing direct competition of right and wrong dNTP substrates with steady state and pre-steady state kinetics. *Biochemistry* **49**, 20–28.
- Johnson KA (1995) Rapid quench kinetic analysis of polymerases, adenosinetriphosphatases, and enzyme intermediates. *Methods Enzymol* **249**, 38–61.
- Mizrahi V, Benkovic P & Benkovic SJ (1986) Mechanism of DNA polymerase I: exonuclease/polymerase activity switch and DNA sequence dependence of pyrophosphorolysis and misincorporation reactions. *Proc Natl Acad Sci USA* **83**, 5769–5773.
- Mizrahi V, Benkovic PA & Benkovic SJ (1986) Mechanism of the idling-turnover reaction of the large (Klenow) fragment of *Escherichia coli* DNA polymerase I. *Proc Natl Acad Sci USA* **83**, 231–235.
- Mizrahi V & Benkovic SJ (1988) The dynamics of DNA polymerase-catalyzed reactions. *Adv Enzymol Relat Areas Mol Biol* **61**, 437–457.
- Mizrahi V, Henrie RN, Marlier JF, Johnson KA & Benkovic SJ (1985) Rate-limiting steps in the DNA polymerase I reaction pathway. *Biochemistry* **24**, 4010–4018.
- Joyce CM (2010) Techniques used to study the DNA polymerase reaction pathway. *Biochim Biophys Acta* **1804**, 1032–1040.
- Schwartz JJ & Quake SR (2009) Single molecule measurement of the ‘speed limit’ of DNA polymerase. *Proc Natl Acad Sci USA* **106**, 20294–20299.
- Seville M, West AB, Cull MG & McHenry CS (1996) Fluorometric assay for DNA polymerases and reverse transcriptase. *Biotechniques* **21**, 664, 666, 668, 670, 672.
- Tveit H & Kristensen T (2001) Fluorescence-based DNA polymerase assay. *Anal Biochem* **289**, 96–98.
- Ma CB, Tang ZW, Wang KM, Tan WH, Li J, Li W, Li ZH, Yang XH, Li HM & Liu LF (2006) Real-time monitoring of DNA polymerase activity using molecular beacon. *Anal Biochem* **353**, 141–143.
- Yu LM, Hu GL & Howells L (2002) Fluorescence-based, high-throughput DNA polymerase assay. *Biotechniques* **33**, 938–941.
- Griep MA (1995) Fluorescence recovery assay: a continuous assay for processive DNA polymerases applied specifically to DNA polymerase III holoenzyme. *Anal Biochem* **232**, 180–189.
- LePecq JB & Paoletti C (1967) A fluorescent complex between ethidium bromide and nucleic acids. Physical-chemical characterization. *J Mol Biol* **27**, 87–106.
- Morgan AR, Lee JS, Pulleyblank DE, Murray NL & Evans DH (1979) Review: ethidium fluorescence assays. Part I. Physicochemical studies. *Nucleic Acids Res* **7**, 547–569.
- Morgan AR, Evans DH, Lee JS & Pulleyblank DE (1979) Review: ethidium fluorescence assays. Part II. Enzymatic studies and DNA–protein interactions. *Nucleic Acids Res* **7**, 571–594.
- Purohit V, Grindley ND & Joyce CM (2003) Use of 2-aminopurine fluorescence to examine conformational changes during nucleotide incorporation by DNA polymerase I (Klenow fragment). *Biochemistry* **42**, 10200–10211.
- Frey MW, Sowers LC, Millar DP & Benkovic SJ (1995) The nucleotide analog 2-aminopurine as a spectroscopic probe of nucleotide incorporation by the Klenow fragment of *Escherichia coli* polymerase I and bacteriophage T4 DNA polymerase. *Biochemistry* **34**, 9185–9192.
- Holden MJ, Haynes RJ, Rabb SA, Satija N, Yang K & Blasic JR Jr (2009) Factors affecting quantification of total DNA by UV spectroscopy and PicoGreen fluorescence. *J Agric Food Chem* **57**, 7221–7226.



- 25 Koba M, Szostek A & Konopa J (2007) Limitation of usage of PicoGreen dye in quantitative assays of double-stranded DNA in the presence of intercalating compounds. *Acta Biochim Pol* **54**, 883–886.
- 26 Blotta I, Prestinaci F, Mirante S & Cantafora A (2005) Quantitative assay of total dsDNA with PicoGreen reagent and real-time fluorescent detection. *Ann Ist Super Sanita* **41**, 119–123.
- 27 Batchelor R, Hagen D, Johnson I & Beechem J (2003) A fluorescent high-throughput assay for double-stranded DNA: the RediPlate PicoGreen assay. *Comb Chem High Throughput Screen* **6**, 287–291.
- 28 McGowan KB, Kurtis MS, Lottman LM, Watson D & Sah RL (2002) Biochemical quantification of DNA in human articular and septal cartilage using PicoGreen and Hoechst 33258. *Osteoarthritis Cartilage* **10**, 580–587.
- 29 Zipper H, Brunner H, Bernhagen J & Vitzthum F (2004) Investigations on DNA intercalation and surface binding by SYBR Green I, its structure determination and methodological implications. *Nucleic Acids Res* **32**, e103.
- 30 Hadfield SJ & Chalmers RM (2012) Detection and characterization of *Cryptosporidium cuniculus* by real-time PCR. *Parasitol Res* **111**, 1385–1390.
- 31 Boehm D, Herold S, Kuechler A, Liehr T & Laccone F (2004) Rapid detection of subtelomeric deletion/duplication by novel real-time quantitative PCR using SYBR-green dye. *Hum Mutat* **23**, 368–378.
- 32 Abiodun OO, Gbotosho GO, Ajaiyeoba EO, Happi CT, Hofer S, Wittlin S, Sowunmi A, Brun R & Oduola AM (2010) Comparison of SYBR Green I-, PicoGreen-, and [3H]-hypoxanthine-based assays for *in vitro* antimalarial screening of plants from Nigerian ethnomedicine. *Parasitol Res* **106**, 933–939.
- 33 Medina RA, Rojas M, Tuin A, Huff S, Ferres M, Martinez-Valdebenito C, Godoy P, Garcia-Sastre A, Fofanov Y & SantaLucia J Jr (2011) Development and characterization of a highly specific and sensitive SYBR green reverse transcriptase PCR assay for detection of the 2009 pandemic H1N1 influenza virus on the basis of sequence signatures. *J Clin Microbiol* **49**, 335–344.
- 34 Cosa G, Focsaneanu KS, McLean JR, McNamee JP & Scaiano JC (2001) Photophysical properties of fluorescent DNA-dyes bound to single- and double-stranded DNA in aqueous buffered solution. *Photochem Photobiol* **73**, 585–599.
- 35 Dragan AI, Casas-Finet JR, Bishop ES, Strouse RJ, Schenerman MA & Geddes CD (2010) Characterization of PicoGreen interaction with dsDNA and the origin of its fluorescence enhancement upon binding. *Biophys J* **99**, 3010–3019.
- 36 Singer VL, Jones LJ, Yue ST & Haugland RP (1997) Characterization of PicoGreen reagent and development of a fluorescence-based solution assay for double-stranded DNA quantitation. *Anal Biochem* **249**, 228–238.
- 37 Tolun G & Myers RS (2003) A real-time DNase assay (ReDA) based on PicoGreen fluorescence. *Nucleic Acids Res* **31**, e111.
- 38 Kuchta RD, Benkovic P & Benkovic SJ (1988) Kinetic mechanism whereby DNA polymerase I (Klenow) replicates DNA with high fidelity. *Biochemistry* **27**, 6716–6725.
- 39 Kuchta RD, Cowart M, Allen D & Benkovic SJ (1988) Kinetic and structural investigations of the replicative fidelity of the Klenow fragment. *Biochem Soc Trans* **16**, 947–949.
- 40 Dahlberg ME & Benkovic SJ (1991) Kinetic mechanism of DNA polymerase I (Klenow fragment): identification of a second conformational change and evaluation of the internal equilibrium constant. *Biochemistry* **30**, 4835–4843.
- 41 Eger BT & Benkovic SJ (1992) Minimal kinetic mechanism for misincorporation by DNA polymerase I (Klenow fragment). *Biochemistry* **31**, 9227–9236.
- 42 Benkovic SJ & Cameron CE (1995) Kinetic analysis of nucleotide incorporation and misincorporation by Klenow fragment of *Escherichia coli* DNA polymerase I. *Methods Enzymol* **262**, 257–269.
- 43 Joyce CM & Grindley ND (1983) Construction of a plasmid that overproduces the large proteolytic fragment (Klenow fragment) of DNA polymerase I of *Escherichia coli*. *Proc Natl Acad Sci USA* **80**, 1830–1834.
- 44 Joyce CM, Kelley WS & Grindley ND (1982) Nucleotide sequence of the *Escherichia coli* polA gene and primary structure of DNA polymerase I. *J Biol Chem* **257**, 1958–1964.
- 45 Dragan AI, Bishop ES, Casas-Finet JR, Strouse RJ, Schenerman MA & Geddes CD (2010) Metal-enhanced PicoGreen fluorescence: application to fast and ultra-sensitive pg/ml DNA quantitation. *J Immunol Methods* **362**, 95–100.
- 46 Dragan AI, Bishop ES, Casas-Finet JR, Strouse RJ, Schenerman MA & Geddes CD (2010) Metal-enhanced PicoGreen fluorescence: application for double-stranded DNA quantification. *Anal Biochem* **396**, 8–12.
- 47 Polesky AH, Dahlberg ME, Benkovic SJ, Grindley ND & Joyce CM (1992) Side chains involved in catalysis of the polymerase reaction of DNA polymerase I from *Escherichia coli*. *J Biol Chem* **267**, 8417–8428.
- 48 Segel LA (1988) On the validity of the steady-state assumption of enzyme-kinetics. *Bull Math Biol* **50**, 579–593.